

BRIEF REPORT

10.1002/2014JA019894

Key Points:

- Solar rotation effects are observed in the entire Martian ionosphere <220 km
- Solar rotation effects found in N_mM2 but not in h_mM2
- Solar rotation effects on the Martian and Earth's ionospheres are compared

Correspondence to:

N. Venkateswara Rao,
ionovenki@gmail.com

Citation:

Venkateswara Rao, N., N. Balan, and A. K. Patra (2014), Solar rotation effects on the Martian ionosphere, *J. Geophys. Res. Space Physics*, 119, 6612–6622, doi:10.1002/2014JA019894.

Received 15 FEB 2014

Accepted 9 JUL 2014

Accepted article online 13 JUL 2014

Published online 1 AUG 2014

Solar rotation effects on the Martian ionosphere

N. Venkateswara Rao^{1,2}, N. Balan^{3,4}, and A. K. Patra¹

¹National Atmospheric Research Laboratory, Gadanki, India, ²Department of Physics, Norwegian University of Science and Technology, Trondheim, Norway and Birkeland Centre for Space Science, University of Bergen, Bergen, Norway,

³Department of Physics, National Cheng Kung University, Taiwan, ⁴STE-Lab, Nagoya University, Nagoya, Japan

Abstract We present a detailed investigation of the solar rotation effects on the Martian high-latitude (~63°N–81°N) ionosphere using the electron density (N_e) data measured by Mars Global Surveyor and solar XUV and EUV fluxes measured by SOHO under high (2000–2001), medium (2003), and low (2005) solar activity conditions. A fast Fourier transform spectral analysis method is used to estimate the amplitude of the rotation period in these parameters. This method clearly reveals the presence of solar rotation effects in the Martian ionospheric N_e at all altitudes (90–220 km), peak electron density (N_mM2), and total electron content under the three solar activity conditions. These effects are in phase with the solar UV fluxes (corrected for the Martian orbit). The period of rotation effect (~26 days) is the same at all altitudes, though its amplitude is strongest at the ionospheric M2 peak (~135–140 km, ~3.5–6% of the mean values) and has a secondary enhancement at the M1 peak (~110–115 km). The effect of solar rotation on the M2 peak is larger during medium solar activity (2003) than during high solar activity (2000–2001). The effect, however, is absent in the ionospheric peak height (h_mM2). The rotation effects on Mars are also compared with those on the Earth. Unlike at Mars, the Earth's high-latitude ionosphere shows no clear solar rotation effect, though the effect is observed clearly at lower latitudes.

1. Introduction

The Sun's interaction with planetary bodies through electromagnetic radiation, energetic charged particle emission (solar wind and coronal mass ejection (CME)), and interplanetary magnetic field (IMF) is the primary source for the energetics and dynamics of planetary environments. However, the Sun-planet interactions are quite complex. Several factors such as a planet's distance from the Sun, its chemical composition, and intrinsic magnetic field play key roles in the interactions. In this regard, the Martian upper atmosphere is unique with its photochemistry dominated by a single species (CO₂) and lack of intrinsic magnetic field [Withers, 2009; Haider *et al.*, 2011]. However, a weak and spatially inhomogeneous remnant crustal magnetic field (~10–250 nT at 170 km in the southern hemisphere) was discovered in the Martian upper atmosphere [Acuña *et al.*, 1998; Mitchell *et al.*, 2007], which makes its plasma environment much more interesting than that of planets without any magnetic field (e.g., Venus' ionosphere). Considering these unique characteristics, the Martian plasma and neutral atmospheres can be considered as test beds for better understanding of the Sun-planet relationship.

The ionospheres of the Earth and Mars owe their existence mainly to the extreme ultraviolet (EUV) and X-ray radiation from the Sun. The active regions on the Sun that radiate at these wavelengths, however, are not uniformly distributed in longitude. As the Sun (differentially) rotates about its axis, these active regions also corotate. Accordingly, the radiation observed at the Earth and Mars show temporal variability, the periodicity of which turns out to be a little different for the two planets (27 days for the Earth and 26 days for Mars) due to their orbital characteristics [Hargreaves, 1992].

The Martian ionospheric structure and dynamics below about 200 km altitude are controlled mainly by photochemistry. Above this altitude, transport and plasma dynamics play significant roles [e.g., Shinagawa and Cravens, 1989; Fox, 2004; Němec *et al.*, 2011]. The photochemically driven portion of the Martian ionosphere mainly consists of O₂⁺ ions formed by the photodissociation of CO₂ molecules [Fox, 2004]. The altitude structure of the daytime Martian ionosphere is characterized by two distinct layers in its electron density (N_e) profile. The primary layer, called the M2 layer, has a peak at around 130–140 km altitude with a peak electron density (N_mM2) of ~10¹¹ m⁻³ [e.g., Fox and Yeager, 2006; Withers, 2009]. This layer is formed by the solar EUV radiation at 20–90 nm wavelength [Withers, 2009]. A secondary layer, called the

M1 layer, occurs with its peak at ~ 110 km altitude with a peak density (N_m M1) of 10^9 m^{-3} . While the M2 layer occurs daily with a clear peak, the M1 layer is irregular and occurs sometimes with a peak, ledge, or shoulder [Bougher et al., 2001; Christou et al., 2007; Mendillo et al., 2006; Withers, 2009]. The M1 layer is formed by solar X-ray radiation at $\sim 1\text{--}20$ nm wavelength and also by electron-impact ionization [Fox, 2004]. In the topside ionosphere above the M2 peak, N_e decreases exponentially with altitude [e.g., Duru et al., 2008; Withers, 2009; Némec et al., 2011]. The historical developments and current understanding of the Martian ionosphere, including observational and modeling aspects, have been recently reviewed by Withers [2009] and Haider et al. [2011].

The solar forcing effects on the Martian upper atmosphere and ionosphere have been addressed by several groups [e.g., Hantsch and Bauer, 1990; Breus et al., 2004; Withers and Mendillo, 2005; Nielsen et al., 2006; Lillis et al., 2010; Girazian and Withers, 2013]. Using the N_e profiles obtained from Mars Global Surveyor (MGS) radio occultation experiments, Breus et al. [2004] and Withers and Mendillo [2005] demonstrated that the square of the daytime N_m M2 is proportional to the cosine of solar zenith angle (SZA) as expected from Chapman's theory. Nielsen et al. [2006] also showed a similar dependence of N_m M2 on SZA using a low-frequency topside sounding experiment (Mars Advanced Radar for Subsurface and Ionosphere Sounding). The positive and negative residuals between the observed and predicted values of N_m M2 are found to occur during periods of relatively high and low solar fluxes [e.g., Withers and Mendillo, 2005].

There have been some studies of the solar rotation effect on the Martian thermosphere [Forbes et al., 2006] and ionosphere [Breus et al., 2004; Withers and Mendillo, 2005; Nielsen et al., 2006]. Using the neutral mass density data at 390 km altitude inferred from precise orbit determination of MGS, Forbes et al. [2006] studied the solar rotation effects on the Martian thermosphere under medium solar activity (2003) and compared the results with those obtained simultaneously for the Earth's thermosphere. Breus et al. [2004], Withers and Mendillo [2005], and Nielsen et al., [2006] reported the presence of a solar rotation periodicity in the Martian ionospheric N_m M2 with a period of ~ 26 days. They also showed that there is a phase difference between the solar rotation periodicity in the Martian N_m M2 and that in the solar flux measured at the Earth, which depends on the Earth-Sun-Mars (ESM) angle. However, the earlier studies are confined to the rotation effects on N_m M2. In this paper, we present a detailed investigation of the solar rotation effects on the entire Martian ionosphere (90–220 km) by applying a fast Fourier transform (FFT) spectral analysis technique. The rotation effects on N_e at all altitudes (90–220 km), total electron content (TEC), and on ionospheric peak height (h_m M2) are presented for three levels of solar activity conditions. In addition, the rotation effects on the Martian ionosphere are compared with those on the Earth's ionosphere obtained using the ionosonde data available simultaneously.

2. Data and Analysis

The N_e profiles used in the present study were measured by the radio science experiment on MGS using radio occultation technique [Hinson et al., 1999]. In this technique, radio signals sent from the spacecraft pass through the atmosphere and ionosphere of Mars and are received at the Earth. During their passage, the raypath bends slightly (due to the refraction by the Martian atmosphere and ionosphere) leading to a measurable shift in the received frequency at the Earth. From this, ionospheric N_e is derived. Radio occultation measurements are carried out when the spacecraft rises-from/passes-behind the disk of Mars as seen from the Earth. As the spacecraft position changes, vertical profiles of N_e can be obtained approximately between 80 km and 250 km. However, geometric constraints limit the measurements to solar zenith angle (SZA) between 44° and 136° . Further details about the technique, its applications to MGS, and limitations can be found in Tyler et al. [1992], Hinson et al. [1999], Gurnett et al. [2008], and Withers [2009]. MGS measures several N_e profiles on a given Martian day, which correspond to nearly the same solar zenith angle (SZA), local time, and latitude but for different longitudes. On average, MGS records eight profiles per day, though as many as 12 profiles are recorded on some days. The MGS measurements are confined to northern high latitudes, except in May 1999 when the measurements were made in southern high latitudes. N_e profiles are available for several months each year from 1998 to 2005 at http://atmos.pds.nasa.gov/data_and_services/atmospheres_data/Mars/Mars.html.

For the present study, we use N_e profiles under high (2000–2001), medium (2003), and low (2005) solar activity conditions. Although 2005 is not a minimum of the 11 year solar cycle, we call it “low” since solar

Table 1. MGS Measurement Periods Under High (2000–2001), Medium (2003), and Low (2005) Solar Activity Conditions and Corresponding Information

	2000–2001	2003	2005
Period	1 Nov 2000 to 9 Jan 2001	22 Mar 2003 to 30 May 2003	1 Apr 2005 to 9 Jun 2005
Number of days	70	70	70
Range in SZA (deg)	75.31–86.62	71.08–79.67	75.56–89.22
Range in latitude (°N)	63.42–77.59	69.10–81.00	64.93–71.78
Range in LST	2.76–3.08	2.34–4.13	3.47–4.74
Range in L_5	70.16–110.88	155.92–197.29	185.35–227.32
Mean $F_{10.7}$	171	122	96

activity in this year is relatively lower than that in 2000–2001 and 2003. Table 1 lists the three periods used and the corresponding parameters such as SZA (degrees), latitude (degrees), local time (hours), areocentric longitude L_5 (or position of Mars around the Sun), and mean solar activity index $F_{10.7}$ (at 10.7 cm radio flux). All the N_e profiles used in this study correspond to northern high latitudes where the magnetic field strength is weak [Mitchell *et al.*, 2007], and hence, magnetic anomalies [e.g., Withers *et al.*, 2005] may not have any significant effect on the N_e values. As listed in Table 1, 70 days of data each covering nearly three solar rotation periods (~27 day) are used for the three solar activity conditions. The data correspond to narrow local time sectors at high latitudes in the Northern Hemisphere and cover the entire globe in longitude. The solar zenith angle (SZA) undergoes gradual day-to-day variation. While the data in 2000–2001 and 2003 correspond to the middle portions of high ($F_{10.7} > 150$) and medium ($100 < F_{10.7} < 150$) solar activity levels, the data in 2005 fall toward the upper end of low solar activity ($F_{10.7} < 100$). For the Earth’s ionosphere, the peak electron density (N_mF_2) and peak height (h_mF_2) measured under medium solar activity (2003) at high-latitude and midlatitude locations (Sodankyla and Beijing) are used (http://www.ukssdc.ac.uk/wdcc1/iwgg_menu.html). Both middle and high latitudes are considered because solar activity effects on the Earth’s ionosphere may be weak at high latitudes due to the variability of the strong geomagnetic field.

To characterize the solar rotation, we used solar EUV and XUV fluxes measured by the solar EUV Monitor (SEM) experiment on the Solar Heliospheric Observatory (SOHO) [Judge *et al.*, 1998] located in the vicinity of the Sun-Earth L1 point. The SEM is a transmission grating spectrometer designed to measure absolute solar EUV flux. The SEM team at http://www.usc.edu/dept/space_science/semdatafolder/semdownload.htm provides integrated solar fluxes in EUV (26–34 nm) and XUV (0.1–50 nm) wavelength bands. For our purpose, we used daily averaged values of these fluxes. Since these two wavelength bands are measured covering the full solar disk and they are the primary energy sources for the formation of the Martian and Earth’s ionospheres, their temporal variation can be used as a proxy to characterize the solar rotation for this study. Although the ionization threshold of CO₂ is 90 nm, the exclusion of other wavelengths in the SEM data may not affect the results of our study. In fact, some studies use the 10.7 cm radio flux ($F_{10.7}$) as a proxy for solar UV radiation [e.g., Breus *et al.*, 2004]. The fluxes measured at the Earth are corrected for the Martian orbit considering the ESM angle. For each N_e profile, MGS provides the distance of Mars from the Earth and the Sun and also the Sun-Earth-Mars angles. From these, the ESM angle can be calculated through the law of sines in trigonometry. The angle is positive when the Earth leads Mars and vice versa. Accordingly, the flux measured at the Earth can be corrected to the Martian orbit by shifting it a few days forward or backward depending on the ESM angle and considering the solar rotation period to be 26 days. These fluxes correspond to a fixed distance of 1 AU from the Sun [e.g., Withers and Mendillo, 2005].

We used FFT spectral analysis to bring out the solar rotation periodicity and its amplitude in the Martian ionospheric N_e and solar fluxes. MGS provides ~8 N_e profiles per day covering different longitudes. These profiles are then (arithmetic) averaged to get a daily mean profile (between 90 and 220 km with 1 km height resolution). There are 70 such daily profiles in each solar activity condition. Each time series consisting of 70 profiles of N_e , spaced 1 day apart, are subjected to 128 point FFT through zero padding. The FFT computation is done separately for each height. The daily average values of N_mM2 , h_mM2 , and the solar fluxes are also subjected to FFT, and periods and amplitudes of the solar rotation effect in respective parameters

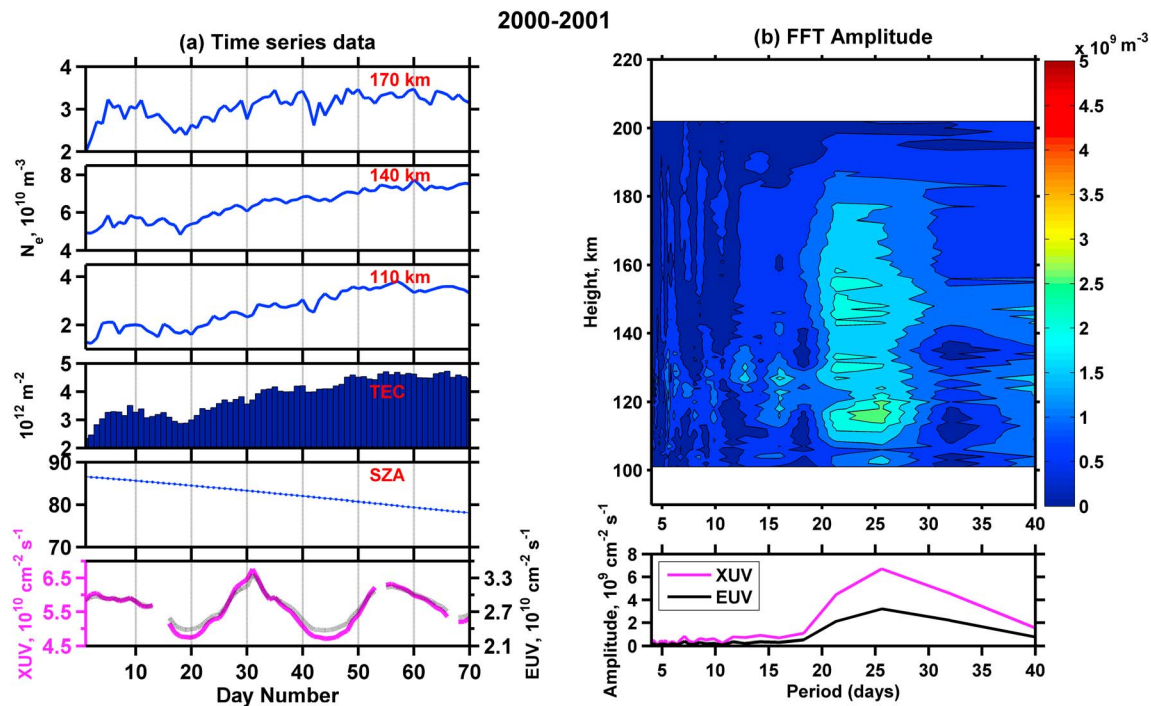


Figure 1. (a) Temporal variation of the daily average N_e at 110 km, 140 km, and 170 km, TEC, SZA, and XUV and EUV fluxes during 1 November 2000 to 9 January 2001, and (b) amplitude spectra of the N_e data at 100–200 km altitude (top) and XUV and EUV fluxes (bottom) for the same period.

are obtained. No special window is used while computing FFT. The analysis is done separately for each parameter and for each solar condition. For the Earth’s ionosphere, N_mF_2 , h_mF_2 , and the A_p index are also subjected to FFT individually and the solar rotation periodicity and amplitudes are estimated.

3. Results

3.1. Altitude Variation of Solar Rotation Effects

Examination of the altitude profiles of individual N_e (figure not shown) at a given longitude shows a time lag of about 2 weeks between the maximal and minimal values. Such variations in N_e may correlate with the solar rotation effect. These variations are observed in all longitudes and under all solar activity conditions, and the effect maximizes around the M2 peak. In the following sections, we study the altitude variation of the solar rotation effect in detail through Figures 1–3 for the three solar activity conditions. Given the fact that the rotation effect is observed in all longitudes, we averaged the N_e profiles at different longitudes over a day for the rest of this study.

3.1.1. High Solar Activity

Though the solar rotation effect on the Martian ionosphere is observed under all solar activity conditions, the effect (in the data we considered) is found to be most distinct under medium (2003) solar activity. However, in the following we present the results in the order of high, medium, and low solar activity conditions. Figure 1 shows the time series data and their amplitude spectra that illustrate the characteristics of the solar rotation effect at high solar activity (2000–2001). The amplitude spectra are calculated using the FFT method (mentioned in section 2). In Figure 1a, first to third rows show the temporal variation of the daily average N_e at three altitudes representing the bottomside ionosphere (110 km), ionospheric peak (140 km), and topside ionosphere (170 km), fourth row gives the corresponding TEC (integrated N_e from 90 to 220 km), fifth row gives the SZA, and sixth row represents the temporal variation of the XUV and EUV fluxes that are corrected for the Martian orbit.

In Figure 1a, the solar rotation effect is apparent in the N_e data in the topside ionosphere (170 km) and in TEC. The rotation effects near the M1 and M2 peaks (110 km and 140 km), however, are masked by the variation

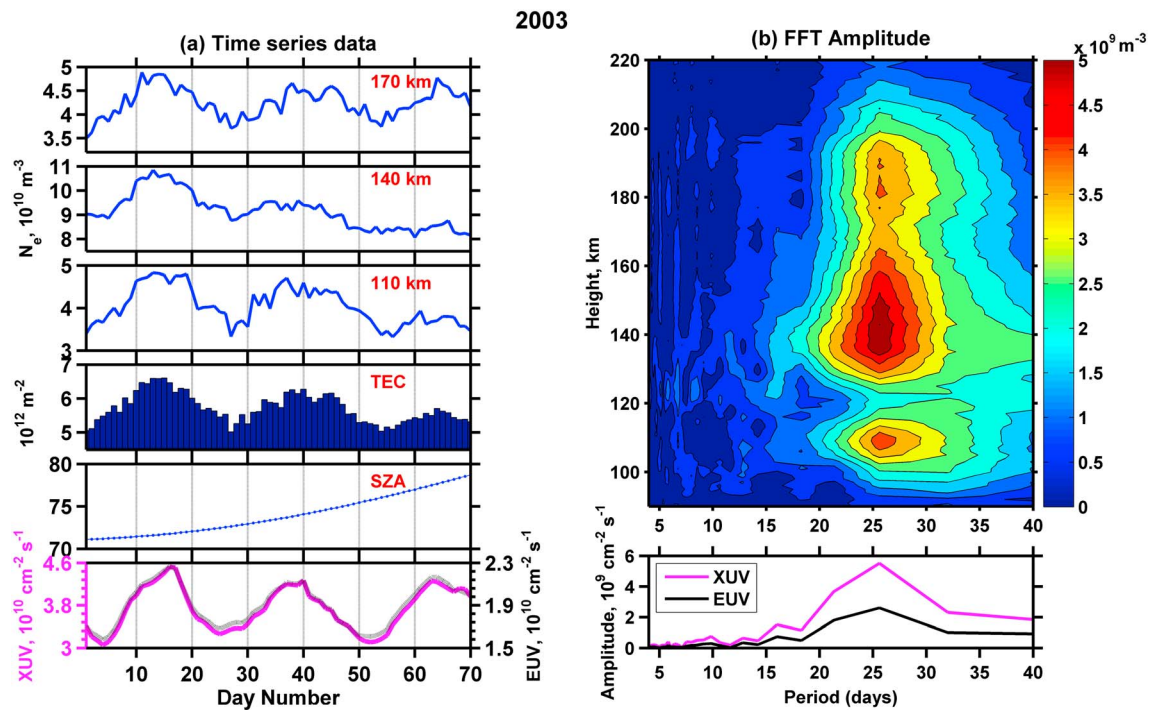


Figure 2. Same as Figure 1 but for 22 March 2003 to 30 May 2003.

of N_e with SZA which changes from $\sim 75^\circ$ to 87° (Figure 1a, fifth row). The spectra in Figure 1b show that the dominant period in N_e and solar flux is nearly equal (~ 26 days), suggesting that the periodicity in N_e is due to solar rotation. The amplitude, however, has a broad maximum between 110 km and 160 km altitude, with the amplitude ($2.8 \times 10^9 \text{ m}^{-3}$) being largest at the M1 peak.

3.1.2. Medium Solar Activity

As mentioned above, the solar rotation effect is found to be most distinct under the medium solar activity (2003), which is illustrated in Figure 2, similar to Figure 1. The N_e at all altitudes (110 km, 140 km, and 170 km) and TEC (Figures 2a) show clear periodic variations with a dominant period of ~ 23 – 27 days centered at ~ 26 days and weak oscillations at shorter periods. The XUV and EUV fluxes also show similar periodic variations suggesting that periodicity in N_e and TEC is due to solar rotation. A gradual decrease of N_e at 110 km and 140 km is also observed, which is due to the increase in SZA from $\sim 71^\circ$ to 80° (Figures 2a, fifth row).

The N_e spectra (Figure 2b, top) show that the solar rotation effect is present at all ionospheric altitudes (~ 90 – 220 km). The dominant period in N_e lies within ~ 23 – 27 days centered at ~ 26 days which is nearly equal to the dominant period in the solar fluxes (Figure 2b, bottom). The solar rotation effect maximizes at the M2 peak (~ 143 km) with an amplitude of $5.2 \times 10^9 \text{ m}^{-3}$, and there is a secondary maximum at the M1 peak (~ 109 km) with an amplitude of $4 \times 10^9 \text{ m}^{-3}$. The amplitude of the solar rotation effect between the M1 and M2 peaks is relatively small.

3.1.3. Low Solar Activity

Figure 3 shows the solar rotation effects under low solar activity (2005). The N_e and TEC variations in this case (Figure 3a) seem dominated by the changes in SZA from $\sim 76^\circ$ to 89° (fifth row), especially near the M1 and M2 peaks. However, the rotation effect is clear in the amplitude spectra (Figure 3b), which show nearly equal (~ 26 days) dominant periods in N_e and in XUV and EUV. The amplitude in N_e is centered at the M2 peak (~ 135 km) with a value of $3.19 \times 10^9 \text{ m}^{-3}$, and it gradually decreases at higher and lower altitudes.

3.2. Solar Rotation Effects on N_mM2

The N_e and TEC data (Figures 1–3) revealed that while the periodicity (~ 26 days) of solar rotation is present at all ionospheric heights, its amplitude, despite SZA variation, is strongest at around the ionospheric peak. Accordingly, it is worthwhile studying the rotation effect on N_mM2 and h_mM2 . The rotation effect on N_mM2 is

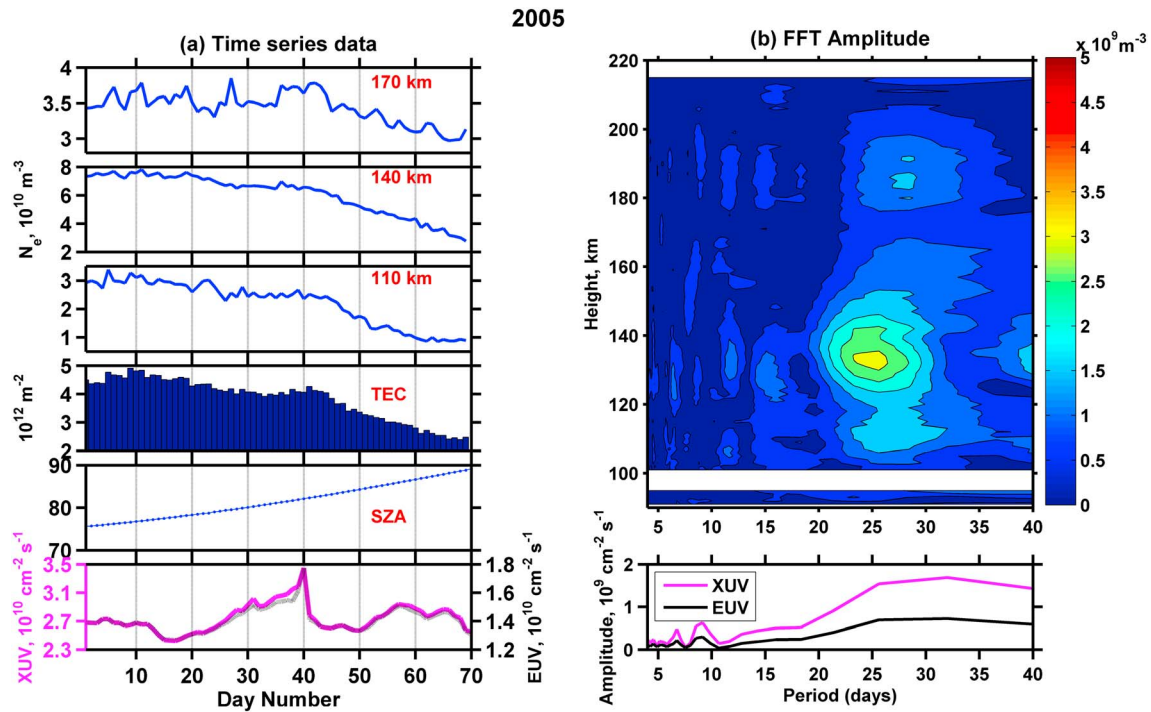


Figure 3. Same as Figure 1 but for 1 April 2005 to 9 June 2005.

shown in Figures 4a–4c for the high, medium, and low solar activity conditions. The SZA contributions on N_mM2 (dotted curves in Figure 4 (top)) are computed by considering the M2 layer as an ideal Chapman layer with peak density (N_m) given by

$$N_m = N_0 \cos^{0.5} \chi \tag{1}$$

where χ is SZA and N_0 is the peak electron density for $\chi = 0$. We assumed N_0 values of $1.9 \times 10^{11} \text{ m}^{-3}$, $1.95 \times 10^{11} \text{ m}^{-3}$, and $1.7 \times 10^{11} \text{ m}^{-3}$ for the high, medium, and low solar activity conditions. These values give

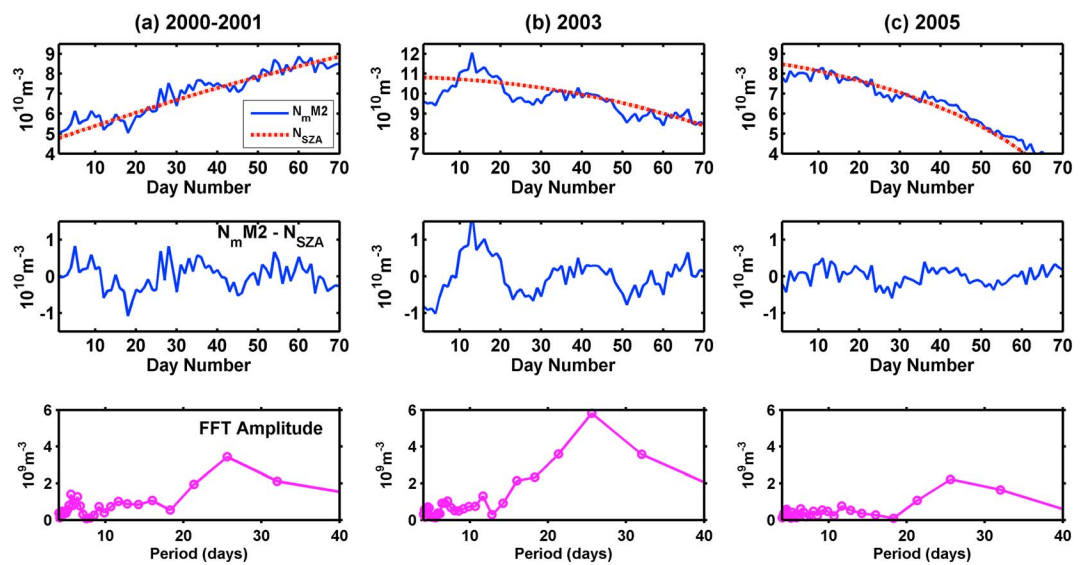


Figure 4. N_mM2 data during (a) 1 November 2000 to 9 January 2001, (b) 22 March to 4 June 2003, and (c) 1 April to 9 June 2005. The first row shows the temporal variation of daily averaged N_mM2 (blue line) and solar zenith angle (SZA) contributions (red curves), the second row shows the difference between the N_mM2 and that from SZA contribution, and the third row displays the amplitude spectra.

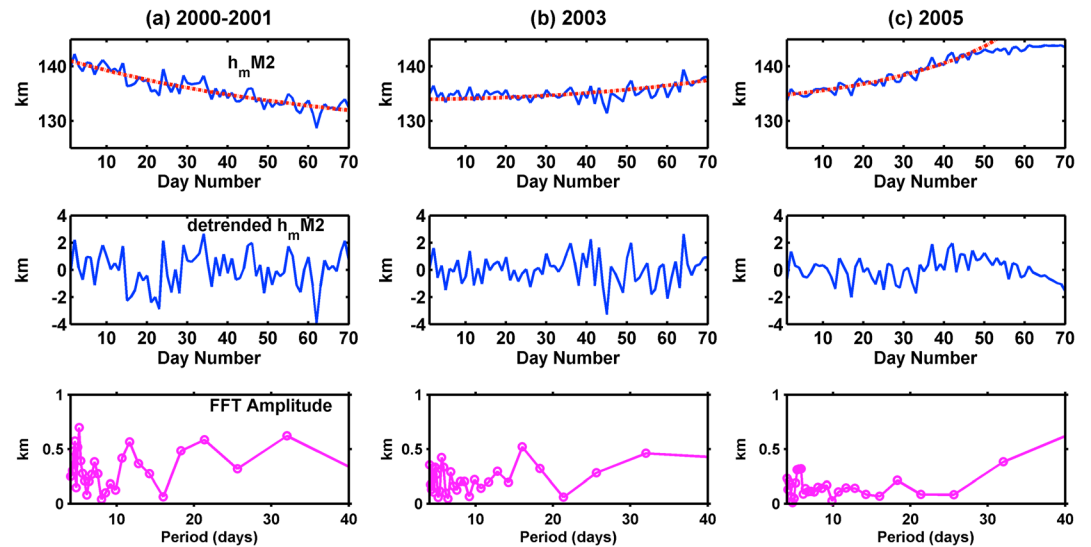


Figure 5. h_mM2 data during (a) 1 November 2000 to 9 January 2001, (b) 22 March to 4 June 2003, and (c) 1 April to 9 June 2005. The first row shows the temporal variation of daily averaged h_mM2 (blue line) and solar zenith angle (red curves), the second row shows the difference between the h_mM2 and that from SZA contribution, and the third row shows the amplitude spectra of h_mM2 .

best fits to the N_mM2 data and are close to the values reported by *Hantsch and Bauer* [1990]. The difference between the observed N_mM2 and SZA contribution (Figure 4, middle) shows a clear solar rotation effect in all three cases with nearly equal periods (~26 days) as in the N_e spectra (Figures 1–3). The amplitudes (Figure 4, bottom) of the solar rotation effect for the three cases are $2.71 \times 10^9 \text{ m}^{-3}$, $5.48 \times 10^9 \text{ m}^{-3}$, and $2.22 \times 10^9 \text{ m}^{-3}$, respectively, which correspond to 3.6%, 5.7%, and 3.5% of the mean densities under the three solar activity conditions. The solar rotation effect (in the data considered) is strongest under medium solar activity.

3.3. Solar Rotation Effects on h_mM2

The temporal variation of the peak height h_mM2 is shown in Figures 5a–5c for the three solar activity conditions. The SZA contribution to h_mM2 (Figure 5, top) is given by

$$h_m = h_0 + H \ln \sec \chi \tag{2}$$

where H is scale height and h_0 is peak height for $\chi = 0$. Best fit for h_m is obtained by varying h_0 between 110 km and 130 km and H between 7 and 13 km. These bounds are close to that given by *Hantsch and Bauer* [1990]. Within these bounds, best fits are obtained for h_0 equal to 120.4 km, 126.10 km, and 121.40 km and H equal to 7.34 km, 7.00 km, and 9.60 km for the three solar activity conditions, respectively. The peak height variation at the end of low solar activity (2005) case is found not to be controlled by SZA. After removing the SZA contribution, some linear trend is still present in h_mM2 which is removed by detrending (removing a linear trend). The detrended h_mM2 is shown in Figure 5 (middle). Interestingly, the solar rotation effect is not observed in h_mM2 . However, it shows fluctuations as large as 6 km within several days. These altitude fluctuations are probably due to atmospheric waves (tides, planetary waves, and gravity waves) propagating from below and changing the altitude of the M2 peak [e.g., *Bougher et al.*, 2001; *Creasey et al.*, 2006; *Lee et al.*, 2009; *Forget et al.*, 2009; *Yiğit et al.*, 2009; *Guzewich et al.*, 2012; *Kleinböhl et al.*, 2013], similar to that in the Earth’s atmosphere [e.g., *Hagan and Forbes*, 2002; *Fritts and Alexander*, 2003; *Venkateswara Rao et al.*, 2008]. The h_mM2 values in Figure 5 (top) are subjected to FFT spectral analysis, and the corresponding amplitude spectra are shown in the bottom. Absence of a peak at ~26 days in the amplitude spectra clearly shows that the solar rotation effects are not observed in h_mM2 .

3.4. Rotation Effects on Earth’s Ionosphere

In addition to solar forcing, the behavior of the Earth’s ionosphere depends on the geomagnetic field and its orientation with respect to the Earth’s surface plane [e.g., *Balan and Bailey*, 1995], which can mask the

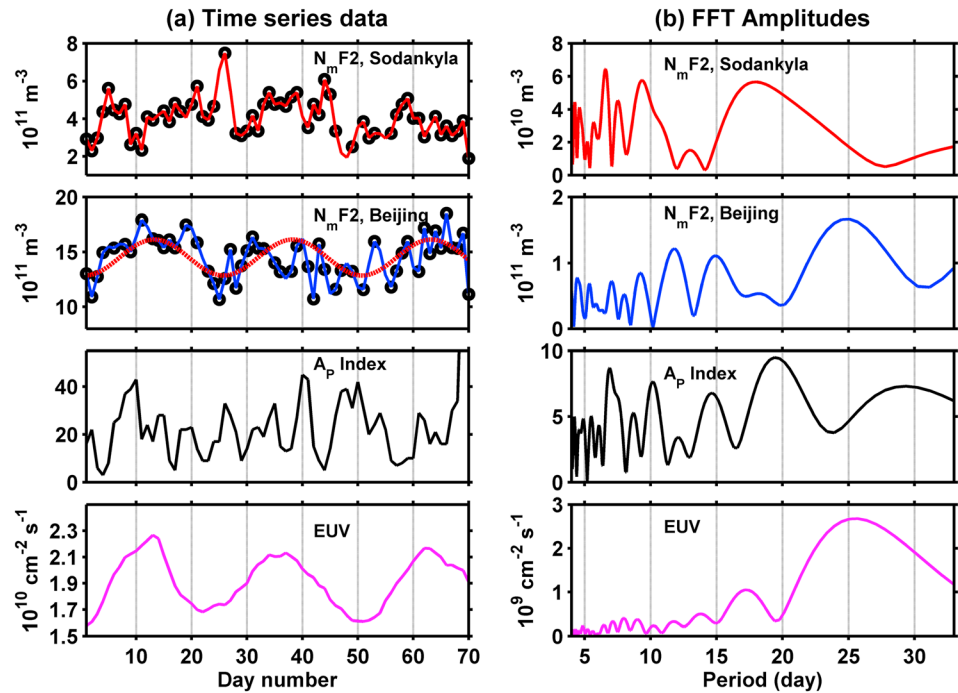


Figure 6. (a) Temporal variations of noontime (11–13 LT) peak electron density ($N_m F_2$) at Sodankyla (67.4°N, 26.6°E; 64°N magnetic latitude) and Beijing (39.9°N, 116.4°E; 34.15°N magnetic latitude); geomagnetic activity index A_p and EUV flux during 22 March to 30 May 2003 and (b) corresponding amplitude spectra.

solar rotation effect especially at high latitudes. There exist several studies on the observations of the 27 day solar rotation period in the Earth’s ionosphere [e.g., Kane *et al.*, 1995; Oinats *et al.*, 2008; Ma *et al.*, 2012]. The solar rotation effect observed on the Martian ionosphere can therefore be appreciated better when it is compared to the effect on the Earth’s ionosphere at different latitudes. We chose the medium solar activity year (2003) for comparison as the solar rotation effects on the Martian ionosphere are clearly observed in this year. Figure 6a (first and second rows) shows the variations of the noontime (11–13 LT) $N_m F_2$ at the high-latitude and midlatitude locations (Sodankyla; 67.4°N, 26.6°E; 64°N geomagnetic latitude; and Beijing; 39.9°N, 116.4°E; 34.15°N geomagnetic latitude) for the period 22 March to 4 June in 2003; the corresponding daily geomagnetic activity index A_p and solar EUV flux are shown in third and fourth rows. The amplitude spectra of these data are shown in the respective rows in Figure 6b.

As shown by the data and spectra, the solar rotation effect is obvious at midlatitudes (Beijing) and $N_m F_2$ has nearly the same dominant period as the EUV flux (~26 days). The amplitude of the dominant period in $N_m F_2$ (at Beijing $\sim 1.6 \times 10^{11} \text{ m}^{-3}$ in 2003) is ~16% of the mean value while the EUV flux fluctuates by ~30%, which suggest that the behavior of the ionosphere depends also on chemical loss and dynamical processes [e.g., Bailey and Balan, 1996]. However, at the high-latitude station (Sodankyla) the dominant period in $N_m F_2$ (~18 days) corresponds to that in A_p . Thus, the solar rotation effects (as expected) are much clearer at the Earth’s midlatitudes than at high latitudes.

4. Discussion

The solar rotation effects on the Martian ionosphere are studied for high (2000–2001), medium (2003), and low (2005) solar activity conditions using the electron density (N_e) data at high latitudes (~63°N–81°N, Table 1) measured by the MGS and solar XUV and EUV flux data measured by SOHO. These data are used to present the rotation effects on N_e in the entire ionosphere (90–220 km), peak electron density ($N_m M2$), peak height ($h_m M2$), and total electron content (TEC). The solar rotation effects on the Earth’s ionosphere are also studied for high and middle latitudes.

The observations show clear solar rotation effects on the Martian ionosphere under low, medium, and high solar activity conditions. The waxing and waning of N_e correlates well with those of the solar EUV and X-ray fluxes (Figures 1–3) indicating that the solar rotation effects are imparted to the Martian ionosphere through photochemistry. The periodicity of the ionospheric response (~ 26 days) is equal to that of the solar fluxes, and the amplitude of the response is centered at the ionospheric peak under the three solar activity conditions, except at high solar activity, when the amplitude at the M1 peak is slightly larger than that at the M2 peak. These observations, in general, seem to agree with those expected from the maximum photoionization rate calculated for 20–90 nm wavelength assuming CO_2 as the dominant neutral species [Fox and Yeager, 2006]. The solar rotation effect also extends to higher altitudes under higher levels of solar activity, which suggests that the photochemically controlled ionospheric region could extend to higher altitudes at higher levels of solar activity [Fox and Yeager, 2006].

However, the rotation effect during medium solar activity (2003, Figure 2) seems to extend to higher altitudes than at high solar activity (Figure 1). Such a peculiarity is also observed in the amplitude of the rotation period, which is stronger at medium solar activity (Figure 2) than at high solar activity (Figure 1). These features can be explained through a combination of the changes in solar activity and the Martian orbit around the Sun. For the Martian orbit, perihelion occurs at $L_s = 250^\circ$ and aphelion occurs at $L_s = 70^\circ$. Considering the Martian eccentricity and its orbit around the Sun, the minimum of N_m M2 occurs at $L_s = 90$ and maximum at $L_s = 255$, with the maximum being 1.16 times the minimum [Gonzalez-Galindo et al., 2013]. In the present study, the mean values of L_s in 2000–2001, 2003, and 2005 are 94, 176, and 206, respectively, while the solar activity gradually decreases ($F_{10.7}$ is 171 in 2000–2001, 122 in 2003, and 96 in 2005). This shows that although 2000–2001 corresponds to high solar activity, Mars is at its aphelion, and in 2005 when the solar activity is less, Mars is close to its perihelion. Thus, in 2003 the solar activity and the Martian orbit provide optimum conditions to receive more solar flux, and hence, the solar rotation effect is stronger than those in the other 2 years.

The solar rotation effects, in general, are found to be clear and large in N_m M2 (Figure 4). The amplitudes of the rotation effect in N_m M2 are found to be ~ 3.5 –6% of the mean N_m M2 (Figure 4). The solar rotation effect, however, is absent in h_m M2 (Figure 5). Previous studies have shown that h_m M2 varies with the Sun-Mars distance through expansion/contraction of the lower atmosphere [e.g., Zou et al., 2011; Gonzalez-Galindo et al., 2013]. This implies that changes in solar flux due to solar rotation are inadequate to cause significant expansion/contraction of the Martian lower atmosphere, similar to the Earth's atmosphere. This again indicates that the observed solar rotation effects on the ionosphere are imparted through photoionization and not through expansion/contraction of the atmosphere. At this point, it may be noted that Forbes et al. [2006] reported the solar rotation effects on the Martian thermospheric density and temperature at altitudes (390 km) well above the photochemically controlled ionosphere (90–220 km), which is due to the increase of the O/CO_2 mixing ratio with altitude above the ionosphere [Keating and Bougher, 1992].

While the solar rotation effect is observed in the Martian ionosphere at high latitudes, the effect in the Earth's ionosphere is clear at middle (and lower) latitudes but not at high latitudes (Figure 6). This is because there is no strong magnetic field in the Martian ionosphere (at northern high latitudes) to mask the solar rotation effect arising through photoionization while in the case of the Earth, strong and complicated geomagnetic effects, in terms of charged particle precipitation and electrodynamics, could dominate the weak solar rotation effect at high latitudes where the geomagnetic field lines are open. At middle and lower latitudes where the field lines are closed, the solar wind and IMF are unable to drive the ionosphere under solar quiet conditions, though they can drive it under active conditions such as during the passage of CMEs [e.g., Fuller-Rowell et al., 1994; Balan et al., 2011].

The amplitude of the solar rotation effect is found to be larger in the Earth's ionosphere than in the Martian ionosphere. However, a direct comparison of solar rotation effects between Mars and the Earth is not attempted because the effects are observed at high latitudes for Mars and at midlatitudes for the Earth. Several factors, including the differences in thermospheric composition, density, and magnetic environments of the two planets may play important roles in determining the solar rotation effects. In the Martian thermosphere, CO_2 is the main species which is ionized by the 20–90 nm EUV fluxes [e.g., Fox and Yeager, 2006] while several atomic and molecular species are ionized by EUV and X-ray fluxes in the Earth's thermosphere [e.g., Bailey and Balan, 1996]. Moreover, diffusion plays a significant role in the Earth's

atmosphere in distributing the plasma. The distance of the Earth and Mars from the Sun is also important in deciding the strength of the solar rotation effects.

5. Conclusions

The electron density data measured by the MGS and solar XUV and EUV fluxes measured by SOHO under high (2000–2001), medium (2003), and low (2005) solar activity conditions are used to study the solar rotation effects on the Martian ionosphere using the FFT spectral analysis technique. The analysis clearly reveals the presence of solar rotation effects on the Martian high-latitude ionosphere which are in phase with the solar fluxes. The rotation effects are observed in the electron density (N_e), peak electron density (N_mM2), and total electron content (TEC); the effect, however, is absent in the peak height (h_mM2). The period of the rotation effect (26 days) is the same in the entire ionosphere (~90–220 km), though its amplitude is strongest at around the ionospheric peak (~135–140 km, which is ~3.5–6% of the mean values). The amplitude of the solar rotation effect is higher during medium solar activity (2003) than high solar activity (2000–2001). A secondary enhancement of the amplitude at the ionospheric M1 peak is also observed. Unlike at Mars, the Earth's high-latitude ionosphere shows no clear solar rotation effect, though the effect is observed clearly at lower latitudes. This is most likely due to differences in the photochemistry and magnetic environment of the two planets.

Acknowledgments

Authors thank the MGS, SOHO, and UK solar system center teams for the data. N.V. Rao also thanks A. Jayaraman for his valuable suggestions at the initial stages of this work and the National Atmospheric Research Laboratory (India) for supporting his research through a postdoctoral fellowship.

Michael Liemohn thanks Andrey Fedorov and two anonymous reviewers for their assistance in evaluating this paper.

References

- Acuña, M. H., et al. (1998), Magnetic field and plasma observations at Mars: Initial results of the Mars Global Surveyor mission, *Science*, *279*, 1676–1680, doi:10.1126/science.279.5357.1676.
- Bailey, G. J., and N. Balan (1996), A low latitude ionosphere-plasmasphere model, in *STEP Hand Book of Ionospheric Models*, edited by R. W. Schunk, p. 173, Utah State Univ., Logan, Utah.
- Balan, N., and G. J. Bailey (1995), Equatorial plasma fountain and its effects—Possibility of an additional layer, *J. Geophys. Res.*, *100*, 21,421–21,432, doi:10.1029/95JA01555.
- Balan, N., M. Yamamoto, J. Y. Liu, Y. Otsuak, H. Liu and H. Luhr (2011), New aspects of thermospheric and ionospheric storms revealed by CHAMP, *a most popular papers*, *J. Geophys. Res.*, *116*, A07305, doi:10.1029/2010JA0160399.
- Bougher, S. W., S. Engel, D. P. Hinson, and J. M. Forbes (2001), Mars Global Surveyor radio science electron density: Neutral atmosphere implications, *Geophys. Res. Lett.*, *28*, 3091–3094, doi:10.1029/2001GL012884.
- Breus, T. K., A. M. Krymskii, D. H. Crider, N. F. Ness, D. Hinson, and K. K. Barashyan (2004), Effect of the solar radiation in the topside atmosphere/ionosphere of Mars: Mars Global Surveyor observations, *J. Geophys. Res.*, *109*, A09310, doi:10.1029/2004JA010431.
- Christou, A. A., J. Vaubillon, and P. Withers (2007), The dust trail complex of 79P/du Toit–Hartley and meteor outbursts at Mars, *Astron. Astrophys.*, *471*, 321–329.
- Creasey, J. E., J. M. Forbes, and D. P. Hinson (2006), Global and seasonal distribution of gravity wave activity in Mars' lower atmosphere derived from MGS radio occultation data, *Geophys. Res. Lett.*, *33*, L01803, doi:10.1029/2005GL024037.
- Duru, F., D. A. Gurnett, D. D. Morgan, R. Modolo, A. F. Nagy, and D. Najib (2008), Electron densities in the upper ionosphere of Mars from the excitation of electron plasma oscillations, *J. Geophys. Res.*, *113*, A07302, doi:10.1029/2008JA013073.
- Forbes, J. M., S. Bruinsma, and F. G. Lemoine (2006), Solar rotation effects on the thermospheres of Mars and Earth, *Science*, *312*, 1366–1368, doi:10.1126/science.1126389.
- Forget, F., F. Montmessin, J.-L. Bertaux, F. González-Galindo, S. Lebonnois, E. Quémerais, A. Reberac, E. Dimarells, and M. A. López-Valverde (2009), Density and temperatures of the upper Martian atmosphere measured by stellar occultations with Mars Express SPICAM, *J. Geophys. Res.*, *114*, E01004, doi:10.1029/2008JE003086.
- Fox, J. L. (2004), Response of the Martian thermosphere/ionosphere to enhanced fluxes of solar soft X rays, *J. Geophys. Res.*, *109*, A11310, doi:10.1029/2004JA010380.
- Fox, J. L., and K. E. Yeager (2006), Morphology of the near-terminator Martian ionosphere: A comparison of models and data, *J. Geophys. Res.*, *111*, A10309, doi:10.1029/2006JA011697.
- Fritts, D. C., and M. J. Alexander (2003), Gravity wave dynamics and effects in the middle atmosphere, *Rev. Geophys.*, *41*(1), 1003, doi:10.1029/2001RG000106.
- Fuller-Rowell, T. J., M. V. Codrescu, R. J. Moffett, and S. Quegan (1994), Response of the thermosphere and ionosphere to geomagnetic storms, *J. Geophys. Res.*, *99*, 3893–3914, doi:10.1029/93JA02015.
- Girazian, Z., and P. Withers (2013), The dependence of peak electron density in the ionosphere of Mars on solar irradiance, *Geophys. Res. Lett.*, *40*, 1960–1964, doi:10.1002/grl.50344.
- Gonzalez-Galindo, F., J.-Y. Chaufray, M. A. Lopez-Valverde, G. Gilli, F. Forget, F. Leblanc, R. Modolo, S. Hess, and M. Yagi (2013), Three-dimensional Martian ionosphere model: I. The photochemical ionosphere below 180 km, *J. Geophys. Res. Planets*, *118*, 2105–2123, doi:10.1002/jgre.20150.
- Gurnett, D. A., et al. (2008), An overview of radar soundings of the Martian ionosphere from the Mars Express spacecraft, *Adv. Space Res.*, *41*, 1335–1346.
- Guzewich, S. D., E. R. Talaat, and D. W. Waugh (2012), Observations of planetary waves and nonmigrating tides by the Mars Climate Sounder, *J. Geophys. Res.*, *117*, E03010, doi:10.1029/2011JE003924.
- Hagan, M. E., and J. M. Forbes (2002), Migrating and nonmigrating diurnal tides in the middle and upper atmosphere excited by tropospheric latent heat release, *J. Geophys. Res.*, *107*(D24), 4754, doi:10.1029/2001JD001236.
- Haider, S. A., K. K. Mahajan, and E. Kallio (2011), Mars ionosphere: A review of experimental results and modeling studies, *Rev. Geophys.*, *49*, RG4001, doi:10.1029/2011RG000357.
- Hantsch, M. H., and S. J. Bauer (1990), Solar control of the Mars ionosphere, *Planet. Space Sci.*, *38*, 539–542.

- Hargreaves, J. K. (1992), *The Solar Terrestrial Environment: An Introduction to Geospace*, Cambridge Univ. Press, New York.
- Hinson, D. P., R. A. Simpson, J. D. Twicken, G. L. Tyler, and F. M. Flasar (1999), Initial results from radio occultation measurements with Mars Global Surveyor, *J. Geophys. Res.*, *104*, 26,997–27,012, doi:10.1029/1999JE001069.
- Judge, D. L., et al. (1998), First solar EUV irradiance obtained from SOHO by the CELIAS/SEM, *Sol. Phys.*, *177*, 161–173, doi:10.1023/A:1004929011427.
- Kane, R. P., E. R. de Paula, and N. B. Trivedi (1995), Variations of solar EUV, UV and ionospheric foF2 related to the solar rotation period, *Ann. Geophys.*, *13*, 717–723, doi:10.1007/s00585-995-0717-4.
- Keating, G. M., and S. W. Bougher (1992), Isolation of major Venus thermospheric cooling mechanism and implications for Earth and Mars, *J. Geophys. Res.*, *97*, 4189–4197, doi:10.1029/91JA02444.
- Kleinböhl, A., R. John Wilson, D. Kass, J. T. Schofield, and D. J. McCreese (2013), The semidiurnal tide in the middle atmosphere of Mars, *Geophys. Res. Lett.*, *40*, 1952–1959, doi:10.1002/grl.50497.
- Lee, C., et al. (2009), Thermal tides in the Martian middle atmosphere as seen by the Mars Climate Sounder, *J. Geophys. Res.*, *114*, E03005, doi:10.1029/2008JE003285.
- Lillis, R. J., D. A. Brain, S. L. England, P. Withers, M. O. Fillingim, and A. Safaeinili (2010), Total electron content in the Mars ionosphere: Temporal studies and dependence on solar EUV flux, *J. Geophys. Res.*, *115*, A11314, doi:10.1029/2010JA015698.
- Ma, R., J. Xu, W. Wang, and J. Lei (2012), The effect of ~27 day solar rotation on ionospheric F_2 region peak densities (N_mF_2), *J. Geophys. Res.*, *117*, A03303, doi:10.1029/2011JA017190.
- Mendillo, M., P. Withers, D. Hinson, H. Rishbeth, and B. Reinisch (2006), Effects of solar flares on the ionosphere of Mars, *Science*, *311*, 1135–1138.
- Mitchell, D. L., R. J. Lillis, R. P. Lin, J. E. P. Connerney, and M. H. Acuña (2007), A global map of Mars' crustal magnetic field based on electron reflectometry, *J. Geophys. Res.*, *112*, E01002, doi:10.1029/2005JE002564.
- Némec, F., D. D. Morgan, D. A. Gurnett, F. Duru, and V. Truhlik (2011), Dayside ionosphere of Mars: Empirical model based on data from the MARSIS instrument, *J. Geophys. Res.*, *116*, E07003, doi:10.1029/2010JE003789.
- Nielsen, E., H. Zou, D. A. Gurnett, D. L. Kirchner, D. D. Morgan, R. Huff, R. Orosei, A. Safaeinili, J. J. Plaut, and G. Picardi (2006), Observations of vertical reflections from the topside Martian ionosphere, *Space Sci. Rev.*, *126*, 373–388.
- Oinats, A. V., K. G. Ratovsky, and G. V. Kotovich (2008), Influence of the 27-day solar flux variations on the ionosphere parameters measured at Irkutsk in 2003–2005, *Adv. Space Res.*, *42*, 639–644, doi:10.1016/j.asr.2008.02.009.
- Shinagawa, H., and T. E. Cravens (1989), A one-dimensional multispecies magnetohydrodynamic model of the dayside ionosphere of Mars, *J. Geophys. Res.*, *94*, 6506–6516, doi:10.1029/JA094iA06p06506.
- Tyler, G. L., G. Balmino, D. P. Hinson, W. L. Sjogren, D. E. Smith, R. Woo, S. W. Asmar, M. J. Connally, C. L. Hamilton, and R. A. Simpson (1992), Radio science investigations with Mars Observer, *J. Geophys. Res.*, *97*, 7759–7779, doi:10.1029/92JE00513.
- Venkateswara Rao, N., A. K. Patra, T. K. Pant, and S. V. B. Rao (2008), Morphology and seasonal characteristics of low latitude E-region quasi-periodic echoes studied using large database of Gadanki radar observations, *J. Geophys. Res.*, *113*, A07312, doi:10.1029/2007JA012830.
- Withers, P. (2009), A review of observed variability in the dayside ionosphere of Mars, *Adv. Space Res.*, *44*, 277–307.
- Withers, P., and M. Mendillo (2005), Response of peak electron densities in the Martian ionosphere to day-to-day changes in solar flux due to solar rotation, *Planet. Space Sci.*, *53*, 1401–1418.
- Withers, P., M. J. Mendillo, H. Rishbeth, D. P. Hinson, and J. Arkani-Hamed (2005), Ionospheric characteristics above Martian crustal magnetic anomalies, *Geophys. Res. Lett.*, *32*, L16204, doi:10.1029/2005GL023483.
- Yigit, E., A. S. Medvedev, A. D. Aylward, P. Hartogh, and M. J. Harris (2009), Modeling the effects of gravity wave momentum deposition on the general circulation above the turbopause, *J. Geophys. Res.*, *114*, D07101, doi:10.1029/2008JD011132.
- Zou, H., R. J. Lillis, J. S. Wang, and E. Nielsen (2011), Determination of seasonal variations in the Martian neutral atmosphere from observations of ionospheric peak height, *J. Geophys. Res.*, *116*, E09004, doi:10.1029/2011JE003833.